Electronic Supplementary Material (ESI) for Journal of Materials Chemistry A.

Supporting Information for

"Nano-garden Cultivation" for Green Electrocatalysis: Controlled Synthesis of Nature-inspired Hierarchical Nanostructures

Xiaoyu Yan,[a] Yang Zhao,[a] Jasper Biemolt,[b] Kai Zhao,[a] Petrus C. M. Laan,[b] Xiaojuan Chao,[a] and Ning Yan *[ab]

[a] School of Physics and Technology, Wuhan University, Wuhan, China.

[b] Van`t Hoff Institute for Molecular Sciences (HIMS), University of Amsterdam, Amsterdam, The Netherlands. Email: N.yan@uva.nl

This file contains:

1. **Materials synthesis procedures**
2. **Materials characterizations and electrochemical measurement procedures**
3. **Supporting tables and figures**

1. Materials synthesis procedures

All the raw chemicals including $Co(NO_3)_2 \cdot 6H_2O$, NH_4F, $CO(NH_2)_2$ (AR), $NaH_2PO_2 \cdot H_2O$, NaH_2PO_4, Na_2HPO_4 was purchased from Aladdin. H_2SO_4 and KOH were purchased from Sinopharm Chemical Reagent Co., Ltd. Carbon cloth (CC) was provided by fuel cell store. All chemicals were used as received without any further purification. CC was cleaned by ultrasound in concentrated HCl for 30 min, followed by rinsing with sonication in acetone, ethanol and water for 15 min, respectively. Ultrapure water was used in all experiments.

1.1. Growth of various $Co(OH)_2$ nanostructures

Soil/CC. Firstly, $Co(NO_3)_2 \cdot 6H_2O$ (1.164 g), urea (1.2 g) and NH_4F (0.269 g) were dissolved in 20 mL water to form a pink solution which was then vigorous stirred for 20 min. The pink solution and cleaned CC (2×2cm) were transferred into a Teflon-lined stainless autoclave (50 mL). The autoclave was not fully sealed, allowing slow evaporation of water at 90 °C for 10 h in an electric oven. When the autoclave cooled down at room temperature, the carbon cloth with coated $Co(OH)_2$ layer was taken out and washed by plenty of water several times before drying in vacuum oven at 60 °C for 3h.

Sprout/CC. Firstly, Co $(NO_3)_2 \cdot 6H_2O$ (0.7476 g), urea (1.2 g) and NH_4F (0.29 g) were dissolved in 20 mL water to form a pink solution which was then vigorous stirred for 20 min. The pink solution and soil/CC (2 × 2 cm) were transferred into a Teflon-lined stainless autoclave (50 mL). The autoclave was sealed and maintained at 120 °C for 3 h in an electric oven. When the autoclave cooled down at room temperature, the carbon cloth with coated $Co(OH)_2$ sprout was taken out and washed by plenty of water several times before drying in vacuum oven at 60 °C for 5h.

Flake/CC. Firstly, $Co(NO_3)_2 \cdot 6H_2O$ (1.164 g), urea (1.2 g) were dissolved in 20 mL water to form a pink solution which was then vigorous stirred for 20 min. The pink solution and soil/CC (2 × 2 cm) were transferred into a Teflon-lined stainless autoclave (50 mL). The autoclave was sealed and maintained at 120 °C for 22 h in an electric oven, allowing the growth of flakes. When the autoclave cooled down at room temperature, the carbon cloth with coated $Co(OH)_2$ flakes was taken out and washed by plenty of water several times before drying in vacuum oven at 60 °C for 5h.

Stone/CC. Firstly, $Co(NO_3)_2 \cdot 6H_2O$ (1.752 g), urea (1.2 g) were dissolved in 20 mL water to form a pink solution which was then vigorous stirred for 20 min. The pink solution and soil/CC (2 × 2 cm) were transferred into a Teflon-lined stainless autoclave (50 mL). The autoclave was sealed and maintained at 120 °C for 22 h in an electric oven. When the autoclave cooled down at room temperature, the carbon cloth with coated $Co(OH)_2$ stones was taken out and washed by plenty of water several times before drying in vacuum oven at 60 °C for 5h.

Grass/CC. the preparation of grass/CC is in principle the same with that of sprout/CC. we have only extended the hydrothermal synthesis to 12 h to allow the full growth of grass from the sprout.

Leaf/CC and flower/CC

A Pt foil (1 × 1 cm) and an Ag/AgCl electrode were used as the counter and reference electrodes, respectively. The electrodeposition was performed at a constant voltage mode (-1 V vs Ag/AgCl) for 5 min. The as-deposited sample was dried at 80 °C in a vacuum oven. For the preparation of flower/CC, the electrolyte was 0.04 M Co $(NO_3)_2$ while that for leaf/CC was 0.1 M Co $(NO_3)_2$.

1.2. Phosphidation of various $Co(OH)_2$ nanostructures

AS shown, $NaH_2PO_2{\cdot}H_2O$ and $Co(OH)_2$ nanostructure/CC (soil, sprout, flake, stone, grass, leaf or flower) were respectively placed in two small porcelain boats in a quartz tube with Ar gas flow. The porcelain boat with $NaH_2PO_2{\cdot}H_2O$ was put at the upstream side while the other one ($Co(OH)_2$ nanostructure/CC) was placed at downstream side (the mass ratio of $NaH_2PO_2 \cdot H_2O$ and $Co(OH)_2$ was 5:1). The quartz tube was heated up to 300 °C, allowing the thermal decomposition of NaH_2PO_2 and the generation of PH_3 gas. The phosphidation was carried out at 300 ^{o}C for 120 min before cooling down to room temperature.

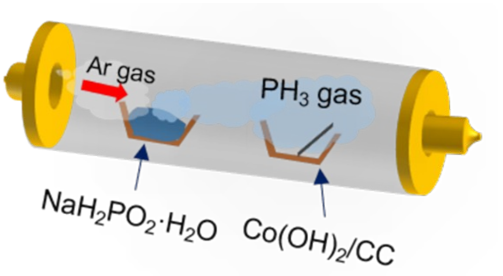

2. Materials characterizations.

XRD measurement was performed by using a D8 Advance X-ray diffractometer with Cu Kα radiation (λ=1.5418 Å) between 5° and 80°. SEM images were taken on a Zeiss Ultra Plus field-emission scanning electron microscope and a FEI Verios 460 field-emission scanning electron microscope, both are coupled with an energy-disperse X-ray spectrometer. TEM and HRTEM images were obtained using a JEM-3010 electron microscrope (JEOL). Sample annealing was conducted in a tube furnace (Tian Central Experimental Furnace Co., Ltd., SK-G05123K). X-ray photoelectron spectroscopy was carried out on a Thermo Fisher ESCALAB 250Xi instrument. The FTIR spectra were obtained on a Bruker Invenio-R spectrometer.

3. Electrochemical tests

Electrochemical measurements were performed using a CHI 760E electrochemical analyzer (CH Instrument Inc.) in a standard three-electrode system using CC, soil/CC, sprout/CC, flake/CC, grass/CC, leaf/CC, flower/CC as the working electrode, respectively. Saturated calomel electrode (SCE) acts as reference electrode. The 0.5 M H_2SO_4, 1.0 M PBS or 1.0 M KOH were used as electrolytes of electrochemical characterization. Linear sweep voltammetry (LSV) and cyclic voltammetry were performed with the scan rate of 5 mV s^{-1}. The Polarization curves were replotted as overpotential (η) vs log current density (log j) to get Tafel plots for quantification of the HER activities of researched catalysts. By fitting the linear portion of the Tafel plots to the Tafel equation ($\eta = b\log(j) + a$).[1, 2] The Tafel slope (b) can be obtained. Chronoamperometry was performed to evaluate the stability of the catalyst. Water splitting electrolyzer in alkaline operated using at two electrode system in a simple glass beaker containing 70 mL of 1 M KOH solution. Two pieces of carbon cloths loaded with same CoP catalysts were served as cathode and anode, respectively.

Table S1. Comparison of the HER activities of CoP flower/CC with selected high-performance electrocatalysts in acidic media (0.5 M H_2SO_4). (η: overpotential at the specified current density)

Catalyst	$\eta_{=10}$ (mV)	$\eta_{=50}$ (mV)	References
$CoSe_2$/CC	190	398	Adv. Mater. 2016, 28, 7527
Co-P-B/CP	172	173	J. Mater. Chem. A, 2018, 6, 6282
r mPF-Co-MoS_2	155	251	Nat. Commun. 2016, 8, 14430
CoMoP@C	133	n.g.	Energy Environ. Sci., 2017, 10, 788
$Fe_{0.9}Co_{0.1}S_2$/CNT	105	146	J. Am. Chem. Soc. 2015, 137, 1587
$NiCo_2Px$/CF	104	150	Adv. Mater. 2017, 29, 1605502
S-MoSe NS	98	113	J. Mater. Chem. A, 2014, 2, 5597–5601
Ni_3S_2@NPC/Cu	92	149	Nano Energy 2017, 36, 85–94
CoP/NPC/TF	91	138	Adv. Energy Mater. 2019, 9, 1803970
Co-Fe-P	86	125	Nano Energy. 2019， 56， 225-233
np-Co_2P	80	119	Adv. Mater. 2016, 28, 2951
FLNPC@MoP-NC/MoP-C/CF	74	148	Adv. Funct. Mater. 2018, 28, 1801527
$Ni_{0.33}Co_{0.67}S_2$/Ti	73	113	Energy Mater. 2015, 5, 1402031
NFP/C-3	72	121	Sci. Adv. 2019, 5, 6009
$FePSe_3$/NC	70	119	Nano Energy. 2019, 57, 222–229
CoP flower/ CC	**68**	**103**	**This work**

Note: n.g. indicates not given or obtainable in the literature.

Table S2. Comparison of the HER activities of CoP flower/CC with selected high-performance electrocatalysts in neutral media (1.0 M PBS).

Catalyst	$\eta_{=10}$ (mV)	$\eta_{=50}$ (mV)	References
CoO/CoSe$_2$/ Ti	337	420	Adv. Sci. 2016, 3, 1500426
Co$_9$S$_8$/CC	175	297	J. Am. Chem. Soc., 2016, 4, 6860-6867
Mo$_x$W$_{2-x}$C@C	152	275	Adv. Mater. Interfaces 2018, 5, 1801302
CoP NA/CC.	145	265	ChemElectroChem 2017, 4,1840 – 1845
FePSe$_3$/NC	140	300	Nano Energy. 2019, 57, 222–229
Co-Fe-P	136	325	Nano Energy. 2019， 56， 225-233
NFP/C-3	117	180	Sci. Adv. 2019, 5, 6009
FLNPC@MoP-NC/MoP-C	106	392	Adv. Funct. Mater. 2018, 28, 1801527
CoP nanowire/CC	106	208	J. Am. Chem. Soc., 2014, 136, 7587-7590
Co-HNP	87	190	Angew. Chem. Int. Ed. 2016, 55, 6725−6729
Mn-Co-P/Ti	86	195	ACS Catal. 2017, 7, 98–102
Ni$_{0.89}$Co$_{0.11}$Se$_2$ MNSN	82	173	Adv. Mater. 2017, 29, 1606521
CoW(OH)x/NF	74	170	ACS Catal. 2018, 8, 5200−5205
CoP flower/ CC	**72**	**138**	**This work**

Table S3. Comparison of the HER activities of CoP flower/CC with selected high-performance electrocatalysts in alkaline media (1.0 M KOH).

Catalyst	η =10 (mV)	η =50 (mV)	References
Co/CoP-5	175	320	Adv. Energy Mater. 2017, 7, 1602355
CoP/Co_2P/Co	160	n.g.	ACS Appl. Mater. Interfaces 2018, 10, 15673
NiS_2–MoS_2 hetero-nanowires	160	210	J. Mater. Chem. A, 2016, 4, 13439–13443
CoS_2 NW	145	190	J. Am. Chem. Soc. 2014, 136, 10053
$CoMoS_3$ nanotubes	133	270	J. Mater. Chem. A, 2017, 5, 11309
$FePSe_3$/NC	118	175	Nano Energy. 2019, 57, 222–229
NFP/C-3	95	150	Sci. Adv. 2019, 5, 6009
CoP/Ti	90	127	Chem. Mater. 2014, 26, 4326
$Ni_{0.33}Co_{0.67}S_2$	88	181	Adv. Energy Mater. 2015, 5, 1402031
V-Ni_2P NSAs/CC	85	275	Nanoscale. 2019, 11, 4198-4203
CoP/NPC/TF	80	148	J. Mater. Chem. A, 2018, 6, 6282
np-$(Co_{0.52}Fe_{0.48})_2$P	79	98	Energy Environ. Sci. 2016, 9, 2257
Mn-Co-P/Ti	76	121	ACS Catal. 2017, 7, 98–102
FLNPC@MoP-NC/MoP-C/CF	69	156	Adv. Funct. Mater. 2018, 28
Co-Fe-P	66	210	Nano Energy. 2019， 56， 225-233
Pt-Ni NWs-S/C	59	n.g.	Nat. Commun. 2017, 8, 14580
CoP flower/ CC	**55**	**91**	**This work**

Note: n.g. indicates not given or obtainable in the literature.

Table S4. Comparison of the OER activities of CoP flower/CC with selected high-performance electrocatalysts in alkaline media (1.0 M KOH).

Catalyst	**$\eta_{=10}$ (mV)**	**$\eta_{=50}$ (mV)**	**References**
NiFe@NC	360	n.g.	Nano Energy .2017, 39, 245–252
p-SnNiFe	350	445	Nat. Commun. 2017, 8, 934
CoMnP	330	n.g.	J. Am. Chem. Soc. 2016, 138, 4006-4009
Co$_4$N	330	370	J. Am. Chem. Soc. 2015, 137, 4119-4125
Poled Co2	320	n.g.	Nat. Commun. 2016, 8, 14430
CoSe$_{0.85}$	300	325	Adv. Mater. 2016, 28, 77-85
CoFe LDH-F	300	n.g.	Adv. Mater. Interfaces. 2019, 10, 1409
boronized Ni	300	330	J. Mater. Chem. A, 2019, 7, 5288-5294
CoFe LDH/NF	300	390	ChemPlusChem 2017, 82, 483
SCFW$_{0.4}$	296	n.g.	J. Mater. Chem. A 2018, 6, 9854-9859
α-Co$_4$Fe(OH)x	295	350	J. Mater. Chem. A 2017, 5, 1078
Zn doped CoO	293	341	ChemCatChem 2019, 11, 1480–1486
CoM-P-3DHFLMs	292	400	Appl. Catal., B 2019, 249 147–154
Amorphous CoSe film	292	351	Chem. Commun. 2015, 51, 16683-16686
Ni$_3$N nanosheets	290	333	Angew. Chem. Int. Ed. 2016, 55, 8670-8674
Ni$_2$P	290	n.g.	Energy Environ. Sci. 2015, 8, 2347-2351.
Co-Bi NS/G nanosheets	290	345	Angew. Chem. Int. Ed. 2016, 55, 2488
p-Cu$_{1-x}$NNi$_{3-y}$/FeNiCu	280	352	Nat. Commun. 2018, 9, 2326
Ni$_3$FeN	280	345	Adv. Energy Mater. 2016, 6, 1502333
CoP flower/CC	**276**	**324**	**This work**

Note: n.g. indicates not given or obtainable in the literature.

Table S5. Comparison of the overall water splitting activities of CoP flower/CC with selected high-performance electrocatalysts in alkaline media (1.0M KOH).

Catalyst	Potential$_{=10}$（V）	Potential$_{=50}$（V）	References
PPy/FeTCPP/Co	1.81	n.g.	Adv. Funct. Mater. 2017, 27, 1606497
NiFeOF/Ni foam	1.80	n.g.	ACS Catal., 2017, 7, 8406–8412
NESSP//NESS	1.74	1.92	Adv. Mater., 2017, 29, 1702095
CC/CNTs@$CoS_{0.74}Se_{0.52}$	1.74	1.88	ChemSusChem 2019, 12,3792 – 3800
CoP/rGO-400	1.70	n.g.	Chem. Sci. 2016, 7, 1690-1695
Co_1Mn_1CH/NF	1.68	1.86	J. Am. Chem. Soc., 2017, 139, 8320–8328
Co_9S_8/WS_2	1.68	1.82	J. Mater. Chem. A, 2017, 5, 23361-23368
$Fe_{0.4}Co_{0.6}$	1.68	1.72	Nano Energy 2017, 38, 576-584
$Co_{0.85}Se$/NiFe-LDH	1.67	n.g.	Energ. Environ. Sci. 2016, 9, 478-483
Ni_3S_2	1.65	1.78	Nanoscale, 2019, 11, 5646-5654
Ni_2Fe_1-O	1.65	1.79	Adv. Energy Mater., 2018, 8
MoS_2-NiS_2/NGF	1.64	n.g.	Appl. Catal., B 2019,254, 15–25
$NiCo_2S_4$-4	1.64	1.78	Adv. Funct. Mater. 2019, 29, 1807031
CoP/NCNHP	1.64	1.77	Adv. Mater. 2019, 31, 1808167
CVN/CC	1.64	1.92	Appl. Catal., B 2019, 241, 521–527
Co-P film	1.64	1.71	Angew. Chem. Int. Edl. 2015, 54, 6251-6254
NiCoFeB	1.81	1.89	Small, 2019, 15, 1804212
Ni foam–supported Ni/Mo_2C (1:2)-NCNFs	1.64	n.g.	Adv. Energy Mater. 2019, 9, 1803185
FCP@NG	1.63	1.83	Nanoscale, 2019, 11, 12837–12845
CoFeZr oxides/NF	1.63	1.75	Adv. Mater. 2019, 31, 1901439
Ni-Pi/CF	1.63	2.15	Adv. Funct. Mater., 2016, 26, 4067–4077
IrP_2/NPC	1.62	1.78	ACS Appl. Mater. Interfaces 2019, 11, 16461-16473
CoP/Ni foam	1.62	1.69	Adv. Funct. Mater., 2015, 25, 7337–7347
CoP flower/CC	**1.61**	**1.71**	**This work**

Note: n.g. indicates not given or obtainable in the literature.

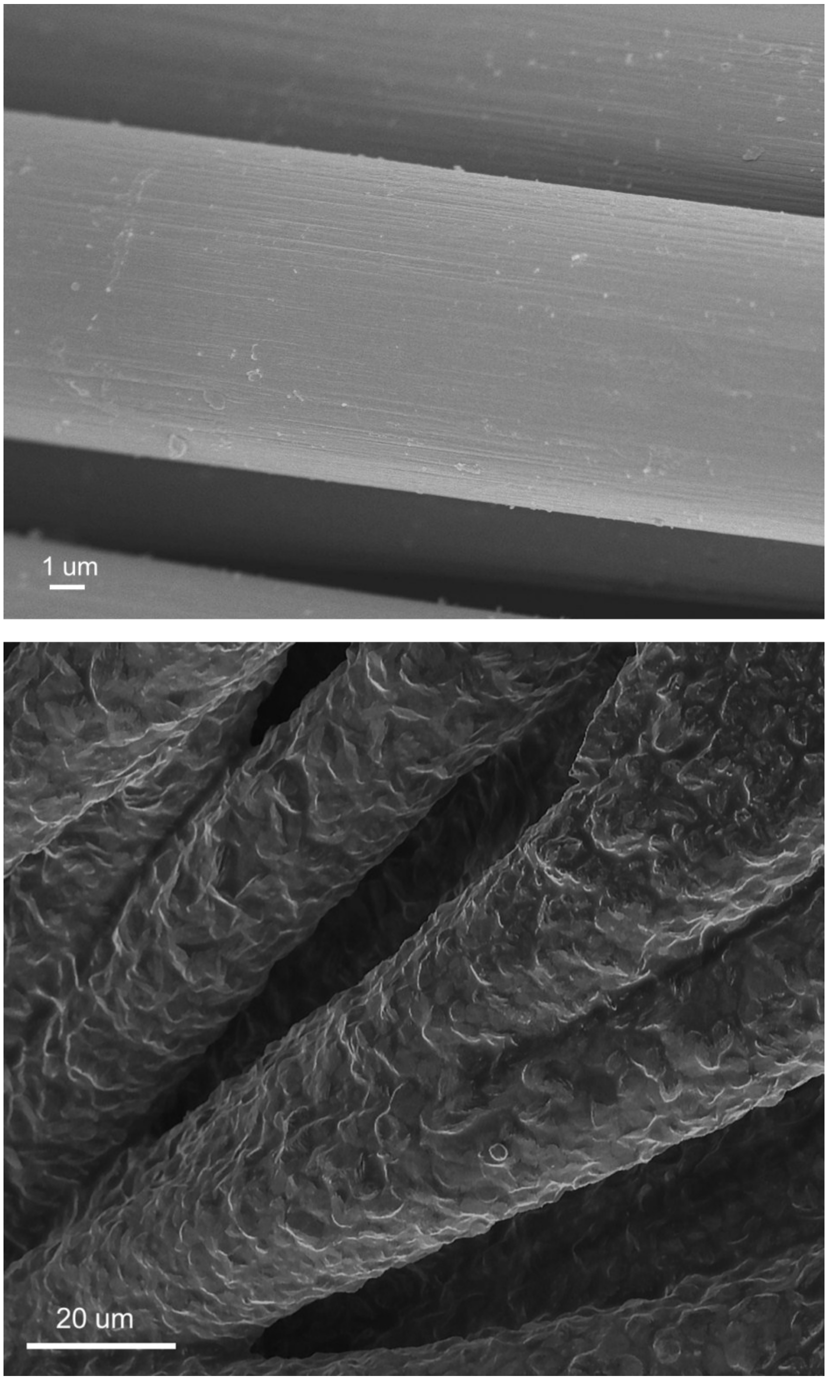

Figure S1. SEM images of (top) pristine and (down) CoP soil layer encapsulated fibers of carbon cloth.

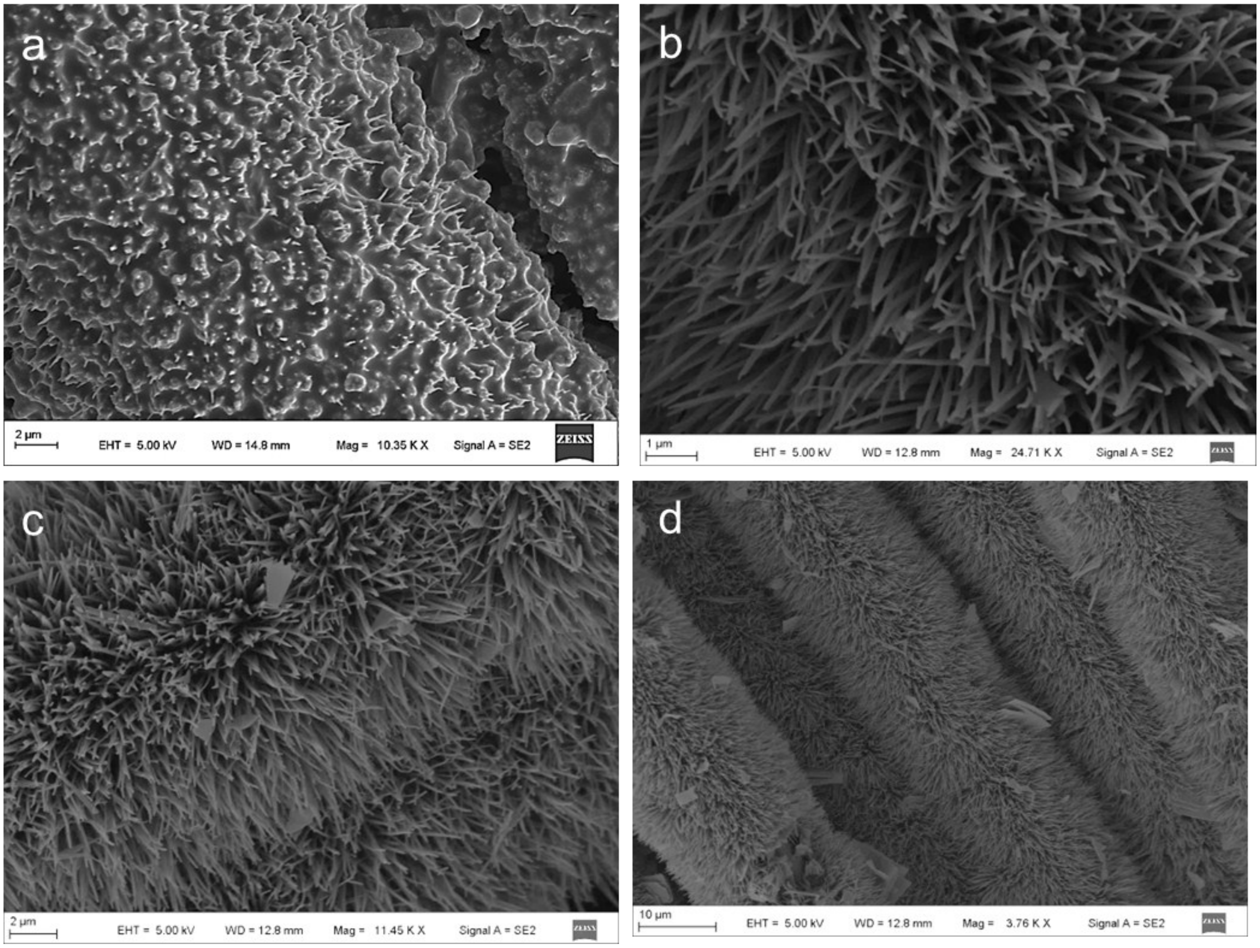

Figure S2. SEM images of (a) sprout and (b-d)grass grown on the soil of carbon cloth.

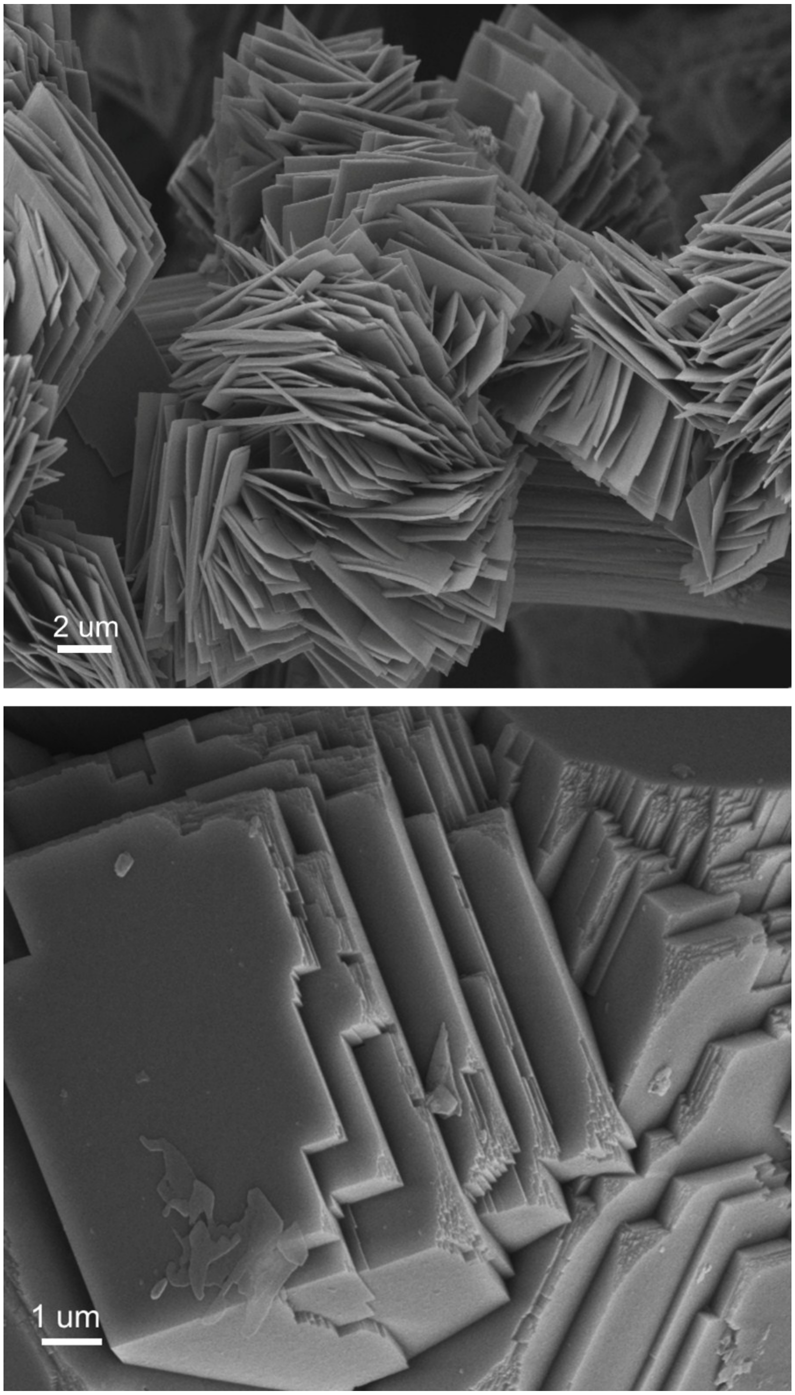

Figure S3. SEM images of (top) lithic flakes and (down) stones on carbon fibers.

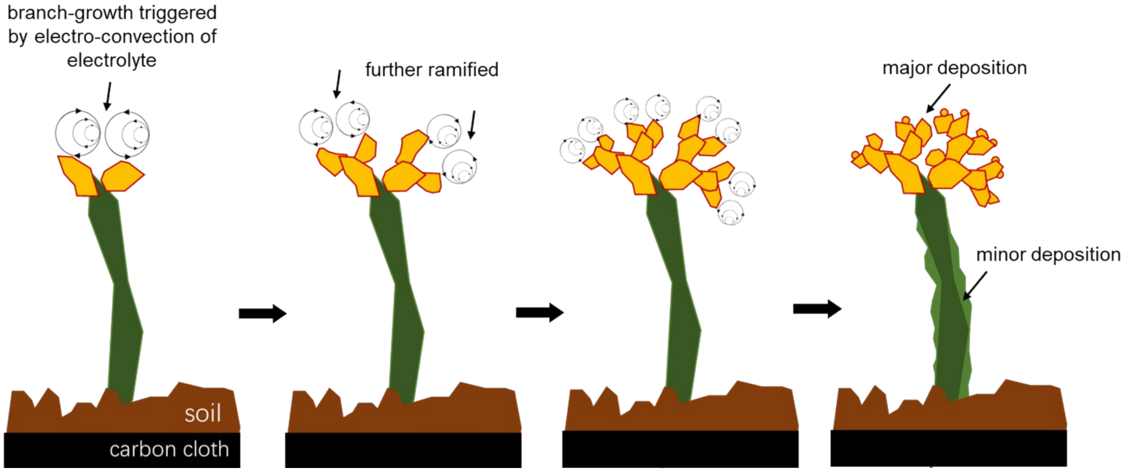

Figure S4. The formation mechanism of the flower on the top of the stem via the branch growth triggered by the electro-convection.

The growth on the tip was initiated by the higher density of space. [3, 4] This simultaneously triggers a convective motion in the electrolyte, can be described quantitatively using the equations developed elsewhere by $v = \nabla \times \boldsymbol{\psi}$, with $\boldsymbol{\psi} = (0, 0, \psi)$ and

$$\psi = v_a x + \frac{s}{48\pi\rho v} f \sum_{k=-\infty}^{k=+\infty} \frac{x - kb}{r_k^2}$$

ρ is the density and ν the viscosity of the liquid, f is the force acting on the liquid, b is the distance between branches, v_a is the speed of the aninos, s is the thickness of the cell, r_k is the distance to the tip of a given tip k and x is the direction perpendicular to the tips.

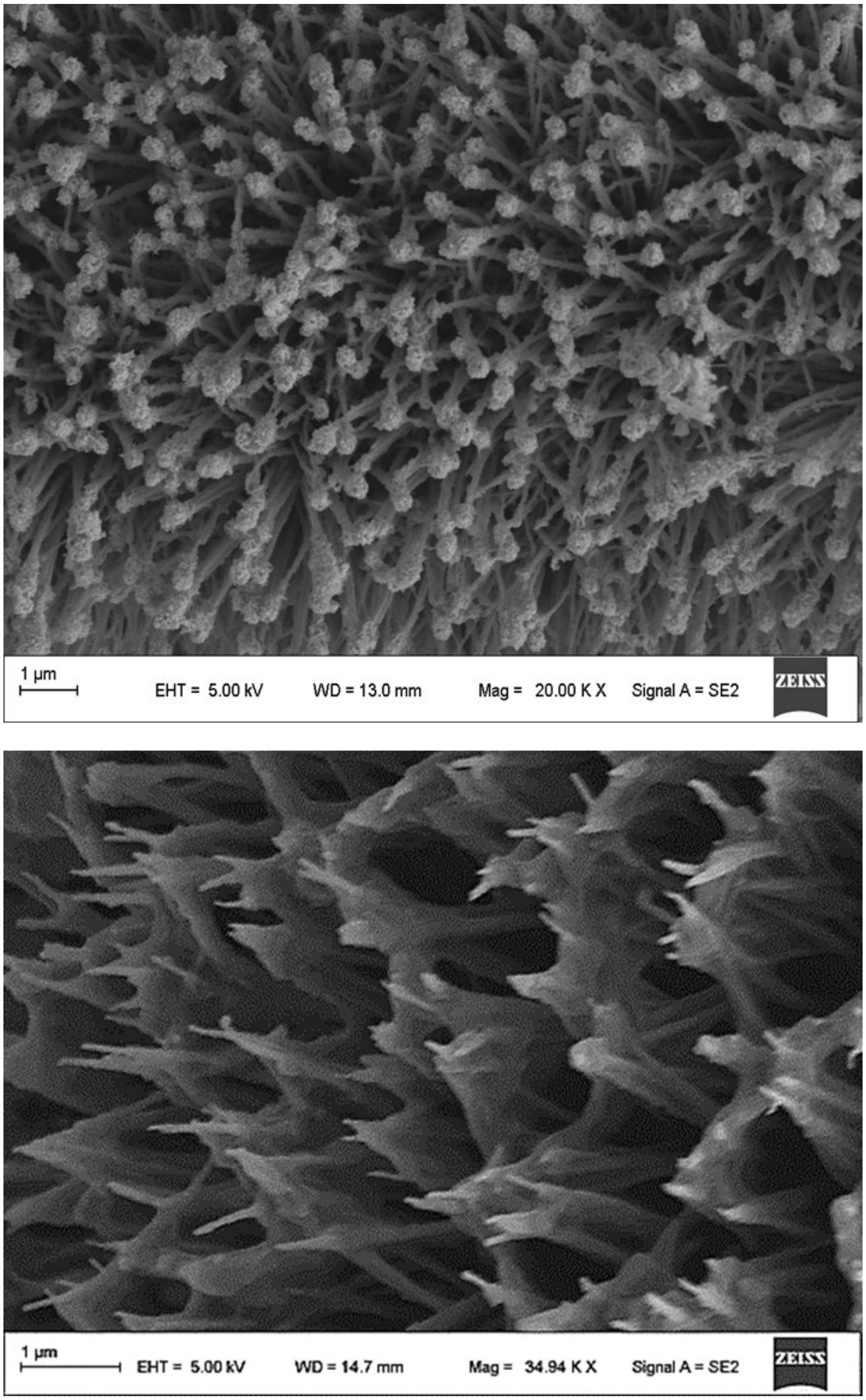

Figure S5. SEM images of (top) flower and (down) leaf CoP nanostructures on the soil layer encapsulated fibers of carbon cloth.

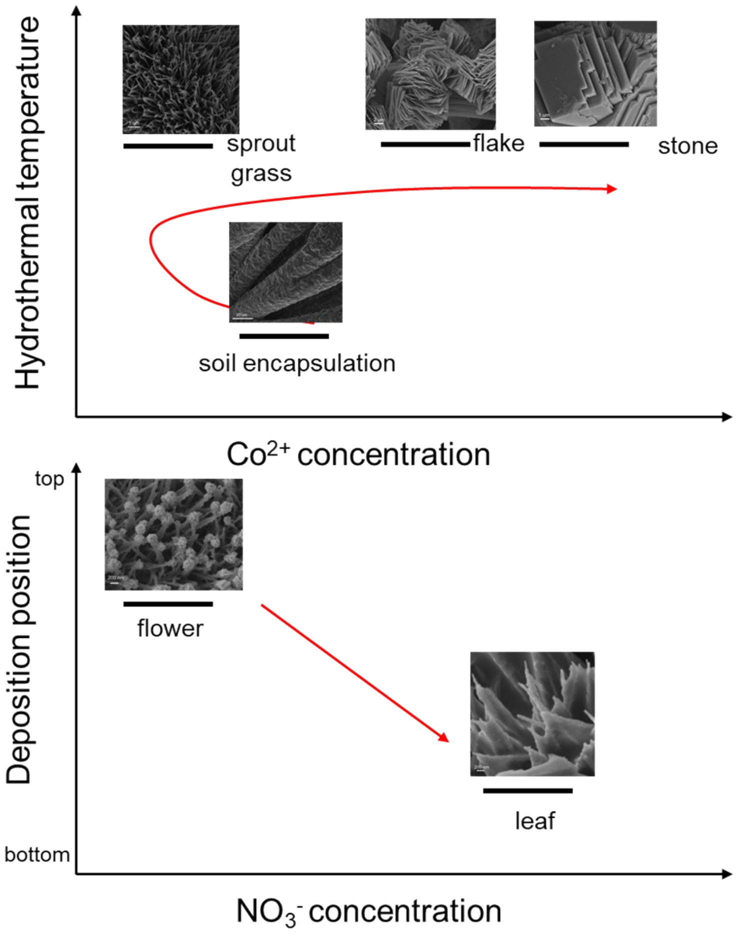

Figure S6. A schematic summary of the controlled synthesis of various nature-inspired nanostructures.

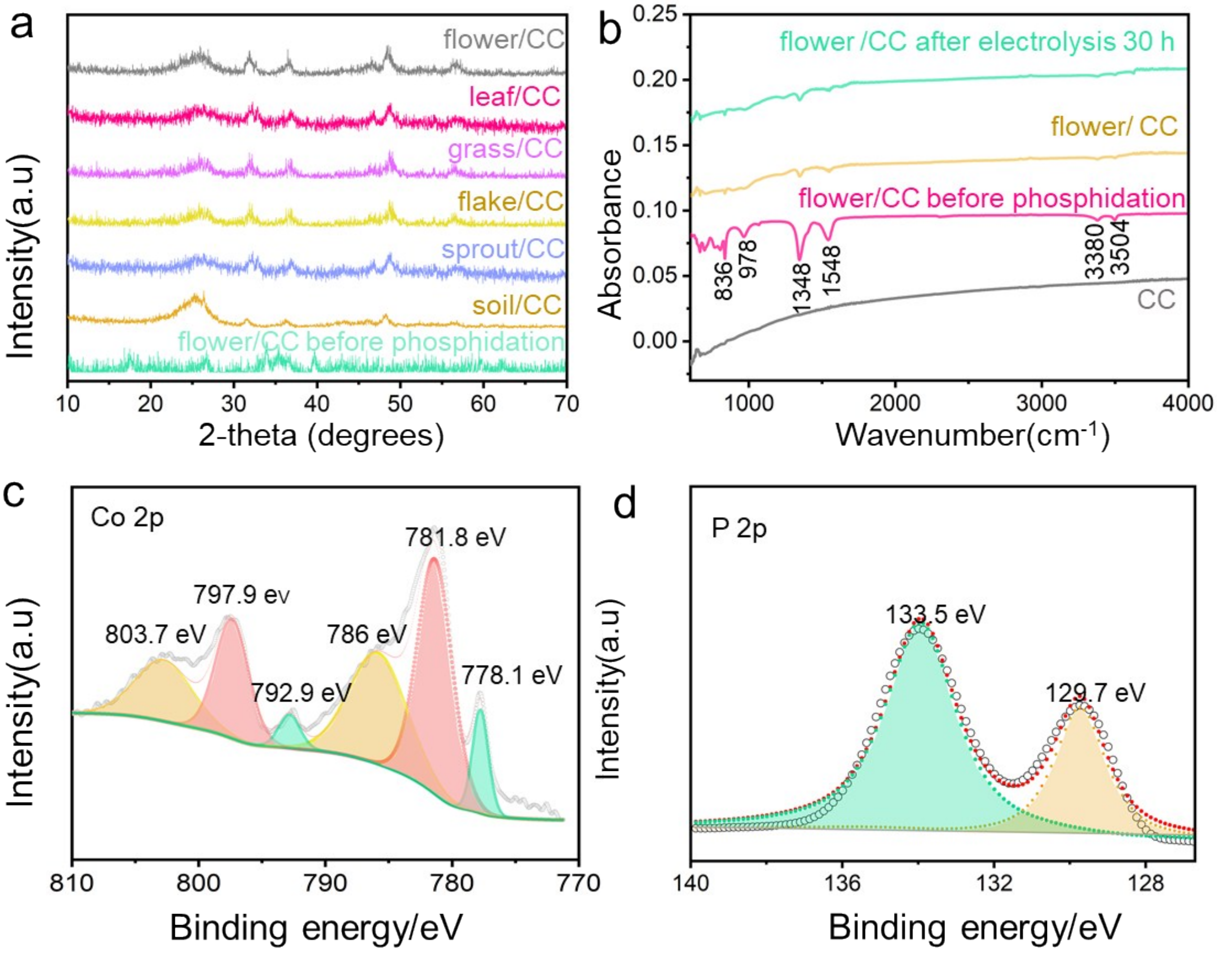

Figure S7. (a) XRD patterns of various nanostructures before and after phosphidation; (b) FTIR spectra of flower/CC before and after phosphidation, and after stability test; XPS spectra of (c) Co 2p and (d) P 2p core level.

In the FTIR spectra, the peaks at 3504 and 3380 cm^{-1} belong to the stretching vibrations of the O–H group of $Co(OH)_{0.44}(CO_3)_{0.78}·0.29H_2O$; The peaks at 1548 cm^{-1}, 1348 cm^{-1} and 836 cm^{-1} are assigned to the characteristic peak of CO_3^{2-}. The peak at 972 cm^{-1} is ascribed to δ(Co–OH) bending mode.[5]

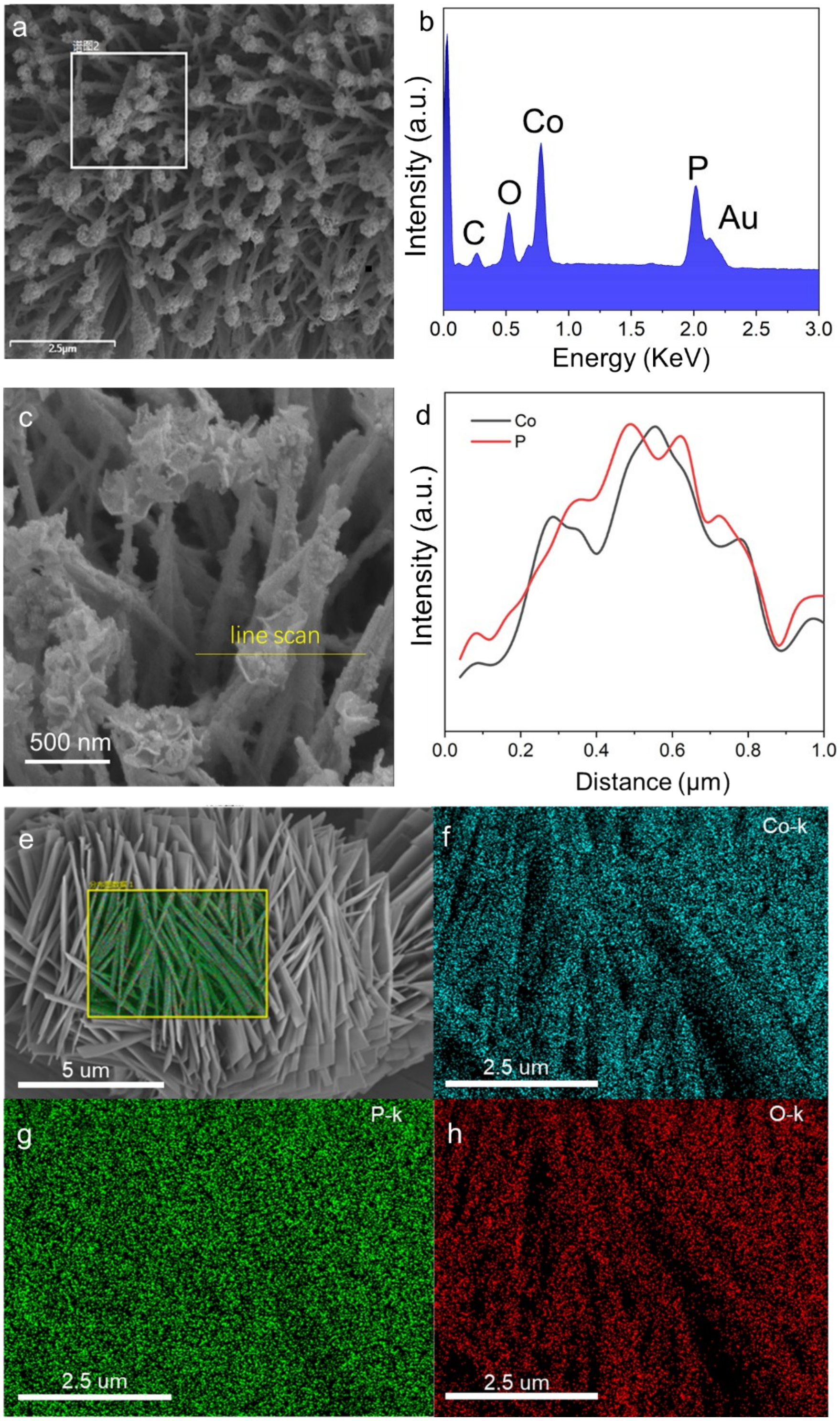

Figure S8. (a) SEM and (b) the corresponding selected area EDX spectrum of flower/CC; (c) HRSEM and (d) the corresponding EDX line scan of the flower and the stem of flower/CC; (e-f) SEM and the corresponding EDX elemental mappings of flake/CC.

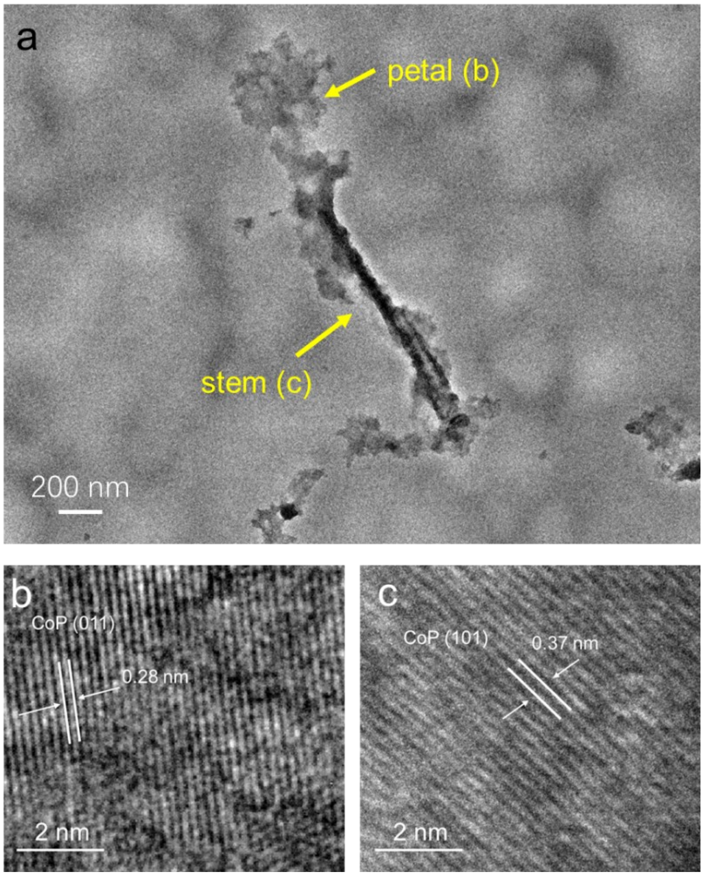

Figure S9. (a) TEM image of flower/CC and the corresponding HRTEM images of the (b) petal and (c) stem part.

To prepare the TEM sample of flower/CC, the flower nanostructure needed to be scratched off the carbon cloth, which caused its partial structural disintegration.

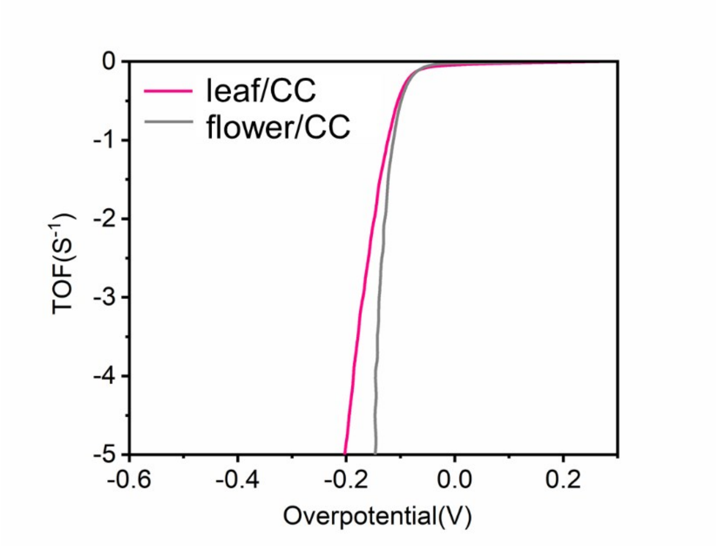

Figure S10. The plot of turnover frequency (TOF) vs overpotential in 0.5 M H_2SO_4.

Assessment of Turnover Frequency (TOF)

We obtained voltammetric charges from CV. Supposing as one electron redox reaction, the whole amount charge was divided by two. To get the numbers of active sites(n), the value was further divided by the Faraday Constant (96485.3 C mol-1)（n=Q/2F）

When we gained the numbers of active sites, the per-site turnover frequencies (in s^{-1}) were calculated by the following equation: [6-8]

$$TOF = I / 2nF \qquad (1)$$

I- the corresponding current density at a certain overpotential of the LSV result.

F- Farady Constant (in 96485.3 C mol^{-1}).

n-Numbers of active sites (in mol).

The factor 1/2 in the equation represents that it takes two electrons to form a hydrogen molecule ($2\ H^+ + 2\ e^- = H_2$).

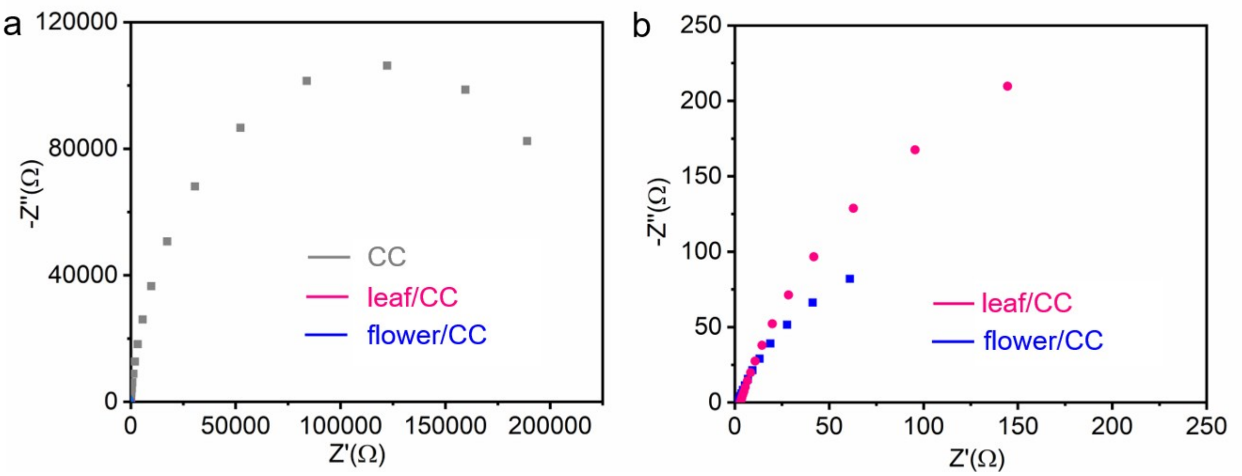

Figure S11. EIS spectra obtained at open-circuit potential in 0.5 M H_2SO_4.

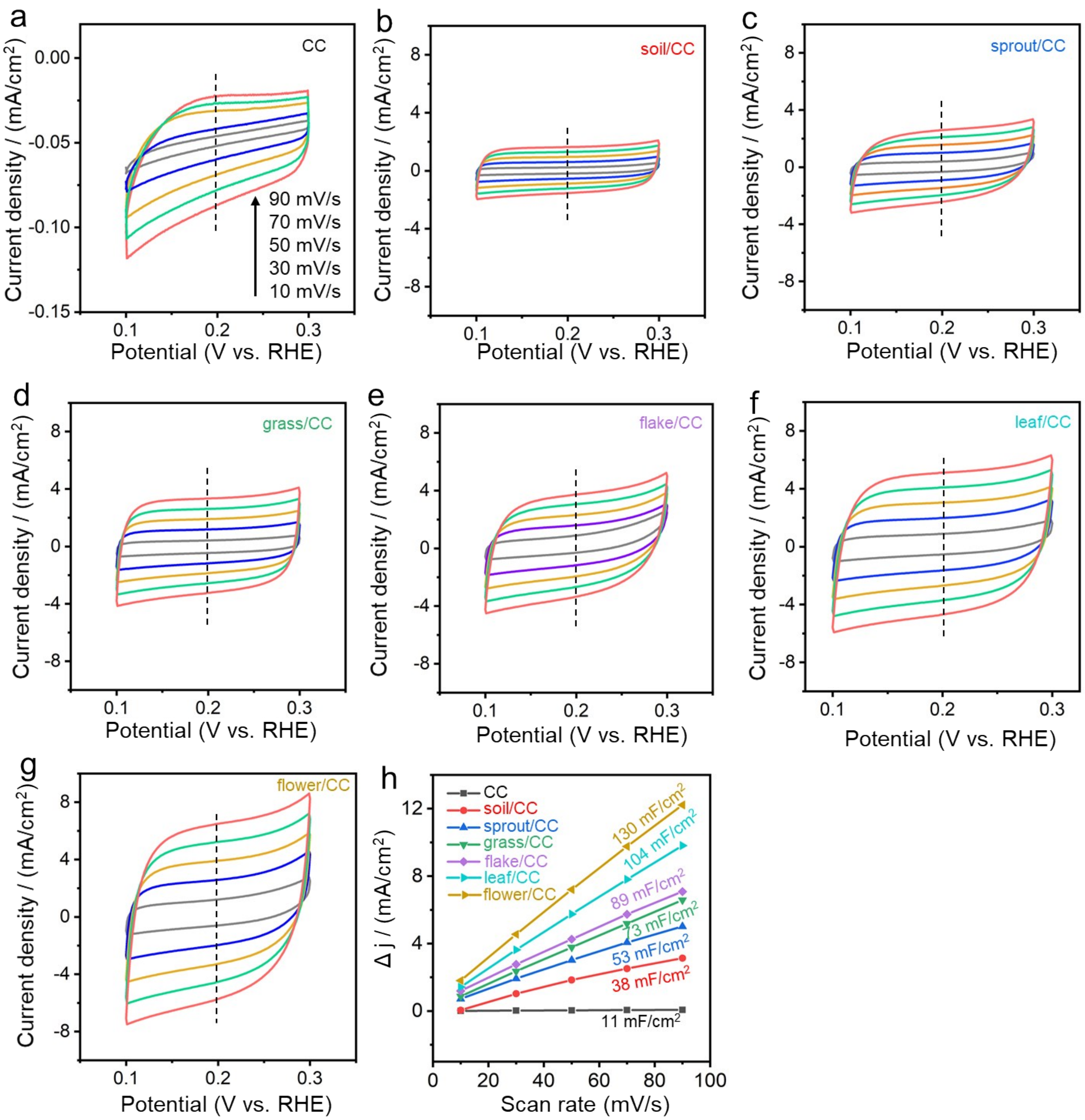

Figure S12. (a-g) CV scans at various scan rate performed in 0.5 M H_2SO_4 aqueous electrolyte of different nanosctructures; (f) the plots of double-layer capacitance that indicate the electrochemically active surface area.

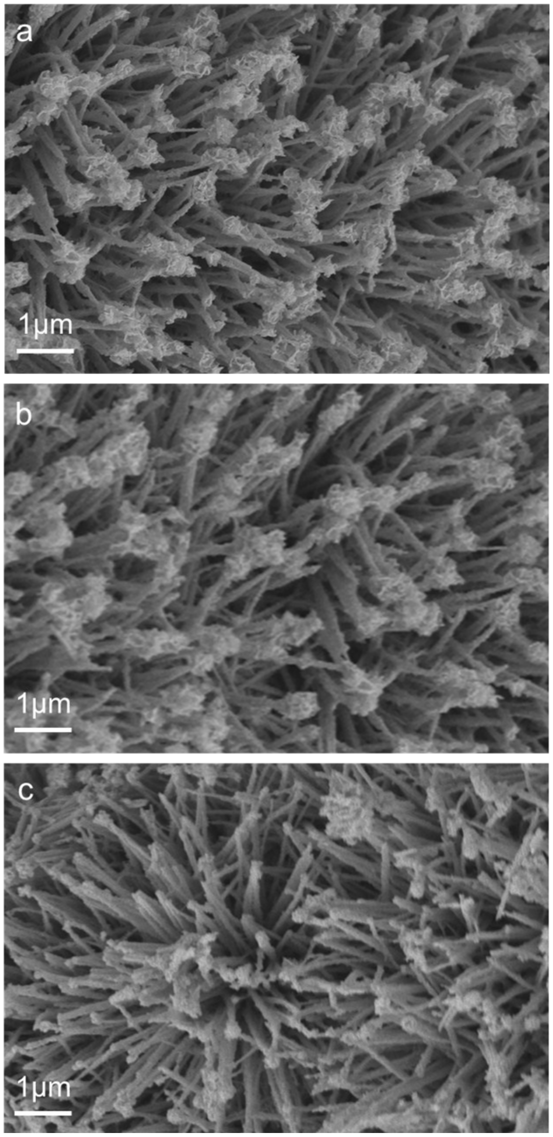

Figure S13. SEM images of and flower/CC after CV stability test in hydrogen evolution reaction in (a) acidic; (b) neutral and (c) alkaline conditions.

References

1. F. Li, L. Zhang, J. Li, X. Lin, X. Li, Y. Fang, J. Huang, W. Li, M. Tian and J. Jin, *J. Power Sources*, 2015, **292**, 15-22.
2. S. Chen, J. Duan, J. Ran and S. Z. Qiao, *Adv. Sci.*, 2015, **2**, 1400015.
3. J.-N. Chazalviel, *PhRvA*, 1990, **42**, 7355-7367.
4. V. Fleury, J.-N. Chazalviel and M. Rosso, *Phys Rev E*, 1993, **48**, 1279-1295.
5. H. Cao, Y. Xie, H. Wang, F. Xiao, A. Wu, L. Li, Z. Xu, N. Xiong and K. Pan, *Electrochim. Acta*, 2018, **259**, 830-840.
6. J. Qian, T. Wang, B. Xia, P. Xi and D. Gao, *Electrochim. Acta*, 2019, **296**, 701-708.
7. J. Guo, X. Zhang, Y. Sun, L. Tang and X. Zhang, *J. Mater. Chem. A*, 2017, **5**, 11309-11315.
8. D. Merki and X. Hu, *Energy Environ. Sci.*, 2011, **4**, 3878-3888.